Quantum corrections to the conductivity in a perovskite oxide: A low-temperature study of $LaNi_{1-x}Co_xO_3$ ($0 \leq x \leq 0.75$)

K. P. Rajeev and A. K. Raychaudhuri
Department of Physics, Indian Institute of Science, Bangalore, 560012, India
(Received 13 December 1991)

In this paper we propose to study the evolution of the quantum corrections to the conductivity in an oxide system as we approach the metal-insulator (M-I) transition from the metallic side. We report here the measurement of the low-temperature (0.1 K $< T <$ 100 K) electrical conductivity of the perovskite-structure oxide system $LaNi_{1-x}Co_xO_3$ ($0 \leq x \leq 0.75$). $LaNiO_3$ is a metal and $LaCoO_3$ is an insulator. The system is metallic for $x \leq 0.65$. For all x, at low temperatures, the conductivity (σ) rises with temperature (T). Below 2 K, σ follows a power-law behavior, $\sigma(T)=\sigma(0)+\alpha T^m$. For samples in the metallic regime, away from the metal-insulator transition ($x \leq 0.4$), $m \approx 0.3$–0.4. As the transition is approached [i.e., $\sigma(0) \to 0$], m increases rapidly; and at the transition [$\sigma(0)=0$, $x_c \approx 0.65$], $m \approx 1$. On the insulating side ($x > 0.65$), m takes on large values and $\sigma(0)=0$. We explain the temperature dependence of $\sigma(T)$, for $T < 2$ K, on the metallic side ($x \leq 0.4$), as arising predominantly from electron-electron interactions, taking into account the diffusion-channel contribution (which gives $m = 0.5$) as well as the Cooper-channel contribution. In this regime, the correction to conductivity, $\delta\sigma(T)$, is a small fraction of $\sigma(T)$. However, as the M-I transition is approached ($x \to x_c$), $\delta\sigma(T)$ starts to dominate $\sigma(T)$ and the above theories fail to explain the observed $\sigma(T)$.

I. INTRODUCTION

The metal-insulator transition in oxides has been studied extensively.[1] In oxides, the metal-insulator (M-I) transition is often composition driven so that it occurs at a certain critical value of the composition. One of the most studied types of oxides is the cubic perovskite-structure compounds, ABO_3, with A standing for a rare-earth, alkali, or alkaline-earth metal and B, a transition metal. In the past, extensive investigations of the chemistry, structure, and structure property correlations were carried out on a number of oxides belonging to this class.[1] The occurrence of high-temperature superconductivity in perovskite-type oxides has given a special significance to the study of these oxides. One of the interesting features of the normal metallic state in these oxides is that they have a rather high electron density ($\sim 10^{22}/\text{cm}^3$) but a low electrical conductivity ($\sigma_{RT} \sim 10^3$–10^4 S/cm) (where RT denotes room temperature). Also, the M-I transition occurs at a very high electron density ($n \sim 10^{21}$–$10^{22}/\text{cm}^3$). The low conductivity and high electron density implies a low electron diffusivity D ($\sim 10^{-1}$–10^{-2} cm^2/s). One would then expect that the systems of this type should show significant quantum corrections to conductivity at low temperatures arising from weak localization and electron-electron interactions. Recently it was shown that, far from the critical composition for M-I transition and well into the metallic state, the diffusivity in these oxides can be low enough so that the electrical conductivity at low temperatures ($T < 4$ K) contains a $T^{1/2}$ term[2–4]—the hallmark of an interacting electron system.[5] It is our principal objective to investigate the extent of applicability of the theories of disordered electronic systems[5] to these oxides. In particular, in these systems one can go from weakly localized to strongly localized regimes. The oxides with their electron densities comparable to those of elemental metals and very low electron diffusivities form a rather unique class of disordered, interacting, electronic systems.

Although the M-I transition in oxides has been studied in the past, very few measurements were carried out at low enough temperatures to study the above-mentioned effects. Only in a very few reports have these questions been even addressed.[3,4,6–8] In the case of perovskite oxides of the type ABO_3, containing transition metals, measurements down to low enough temperatures have only recently begun.[3,4,8] The principal motivation and relevance of the current investigation should be seen in this perspective.

At the outset, it must be said that these oxides, even the simpler ones, can be rather complex if one considers the various interactions present concurrently. In this investigation we make an attempt to analyze the data using the known theories.

In almost all the past studies[1] on the metal-insulator transition in oxides, the transition was determined by the criterion that at the transition, the "metallic" ($d\sigma/dT < 0$) behavior changes to "semiconductorlike" ($d\sigma/dT > 0$), and this generally happens when σ reaches the "minimum" metallic conductivity σ_{Mott} [$\sim(\frac{1}{3}\pi^2)(e^2/\hbar)k_F$]. This criterion has been widely used in the past to find the critical electron density (n_c) at which the M-I transition occurs. With the advent of the scaling theory of localization,[9] it is now clear that the transition can be a continuous one and $d\sigma/dT > 0$ does not necessarily indicate the absence of metallicity [i.e., one can have a $d\sigma/dT > 0$ but $\sigma(T=0) \neq 0$]. It seems

that, in these transition-metal oxides, one has metallic states $[\sigma(T=0)\neq 0]$ for a large range of composition where $d\sigma/dT>0$ and $\sigma<\sigma_{\text{Mott}}$ (see Fig. 3). This implies that the identification of the critical electron density for *M-I* transition with the criteron $\sigma\approx\sigma_{\text{Mott}}$ or with the change of sign of $d\sigma/dT$, overestimates n_c. The proper criterion for the *M-I* transition should be the composition where $\sigma(T=0)\rightarrow 0$. As an example, in the Ta-substituted sodium tungsten bronze ($Na_xTa_yW_{1-y}O_3$), if we use the criterion of the change of sign of $d\sigma/dT$, the critical composition is $(x-y)_c\approx 0.33$. But the true $(x-y)_c$ estimated from the low-temperature conductivity[7,8] using the proper criterion of metallicity $[\sigma(T=0)\neq 0]$ is much lower $[(x-y)_c\approx 0.19]$. We thus find that even for the determination of proper critical concentration n_c for *M-I* transition, measurement of $\sigma(T)$ in the oxide metals should be done at low enough temperatures so that one can get a proper estimate of $\sigma(T=0)$.

The above discussion identifies the motivation for the present investigation. The objectives of this work are to investigate the following issues.

(i) How to do the interaction and localization effects manifest themselves, in the low-temperature electrical conduction, in these oxide metals?

(ii) To what extent are the theories of disordered metallic electronic systems (weak localization and electron-electron interactions theories, collectively known as quantum correction theories) applicable to metallic oxides?

(iii) To investigate the compositions close to the *M-I* transition where the existing quantum correction theories may not apply.

With these objectives we carried out precise measurements of $\sigma(T)$ in the oxide system $LaNi_{1-x}Co_xO_3$ in the temperature range 0.1 to 100 K for $0\leq x\leq 0.75$. We chose this system for the following reasons: (i) this particular system has been investigated before at higher temperatures ($T>20$ K),[10,11] (ii) it does not undergo any crystallographic transformation as the composition is varied,[10] and (iii) it has a simple electronic structure (as will be explained later). In the next section, we present a brief description of certain relevant facts about the system under study.

II. THE SYSTEM $LaNi_{1-x}Co_xO_3$

In this section we present a simple picture of the electronic structure of the system investigated. Pure $LaNiO_3$ is a metallic oxide. The Ni^{3+} in this oxide is in a low spin state ($t_{2g}^6e_g^1$). The conduction band is formed by the hybridization of low-spin nickel e_g orbitals and oxygen p orbitals. Since the t_{2g} band is filled and e_g electrons take part in forming the delocalized σ^* band, the material has no local moments at the Ni^{3+} sites and shows a Pauli-like temperature-independent susceptibility for $T>50$ K (at lower temperatures the susceptibility shows a slight rise[12]). Recently we carried out a detailed investigation of the low-temperature properties of this material.[4] In Table I we give the relevant numbers pertaining to $LaNiO_3$. Along with these numbers, we also give the numbers for copper and $YBa_2Cu_3O_7$. It is seen that the properties of $LaNiO_3$ are rather similar to the normal-state properties of $YBa_2Cu_3O_7$. We see that $LaNiO_3$ may serve as a model for the normal-state properties of many of the oxide metals, normal as well as superconducting (even though some of the high-T_c superconducting oxides have a layered structure and have hole conduction).

While $LaNiO_3$ is metallic, $LaCoO_3$ is an insulator. Co^{3+} is in the low-spin state ($t_{2g}^6e_g^0$) at low enough temperatures ($T\ll 200$ K); the conduction band σ^* (formed by the e_g states and oxygen p orbitals) is empty and the t_{2g} band is full. At higher temperatures ($T>200$ K) the Co ion undergoes a transition to a high-spin state $t_{2g}^4e_g^2$; this populates the σ^* band and the conductivity of the material increases.[12] As the Ni ion in $LaNiO_3$ is substituted by the Co ion, the electron density (and hence E_F) decreases. The substitution of Co also introduces disorder because of the difference in the $3d$ levels $[E^{3d}(\text{Co})-E^{3d}(\text{Ni})\approx 1$ eV]. Most probably, the *M-I* transition in this material occurs in the σ^* band. (The energy-band scheme presented here is based on the one given by Goodenough[13] for ReO_3. It must be admitted that the simple, one-electron-band picture presented here is rather naive. We hope, in light of the recent spate of activities on correlated oxide systems, that a better picture of the electronic conduction in these oxides will soon emerge.) Previous studies[10] on $LaNi_{1-x}Co_xO_3$ have shown that as x is increased, $d\sigma/dT$ (at room temperature) changes sign for $x\approx 0.4$, which corresponds to $n\approx 10^{22}/\text{cm}^3$. (This electron concentration is estimated from the assumption that each Ni^{3+} ion contributes one electron to the conduction band. In the case of pure $LaNiO_3$, this was found to be the case.[4]) For reasons mentioned earlier, we do not identify this as the critical composition for the *M-I* transition. We show below that the *M-I* transition occurs at $x\approx 0.65$ and the correspond-

TABLE I. A comparison of the basic electronic properties of $LaNiO_3$ to those of copper and $YBa_2CU_3O_7$. Please note that for D and k_Fl, the values for 273 K are quoted. Data on $YBa_2Cu_3O_7$ are from Ref. 33. [TCR $=(1/\rho)(d\rho/dT)$, l is the electron mean free path, k_F is the Fermi wave vector, and $m_0=9.1\times 10^{-31}$ kg.]

Property	$LaNiO_3$	$YBa_2Cu_3O_7$	Cu
Electron density n (cm^{-3})	1.7×10^{22}	0.6×10^{22}	8.5×10^{22}
Debye temperature Θ_D (K)	420	370	315
Fermi energy E_F (eV)	0.21	0.12	7
Density of states $g(E_F)$ (eV^{-1} cm^{-3})	1.1×10^{23}	0.7×10^{23}	0.18×10^{23}
Effective mass m_{eff}/m_0 At 273 K	11	9.6	1.3
Diffusivity D (cm^2/s)	3×10^{-2}	4.4×10^{-1}	2.2×10^{2}
TCR (K^{-1})	3.4×10^{-3}	3.7×10^{-3}	4.4×10^{-3}
k_Fl (approximate)	1	11	570

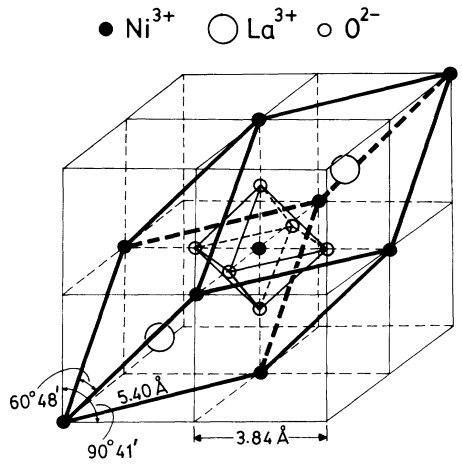

FIG. 1. Crystal structure of $LaNiO_3$. The structure is rhombohedral (trigonal). The unit cell is shown and it has eight formula units, each contained in a small pseudocubic cell. The thick lines indicate the primitive cell, which contains two formula units. Also shown in the figure is the octahedron formed by the *O* ions surrounding a Ni ion. (Only the ions belonging to the primitive cell are shown in the figure.)

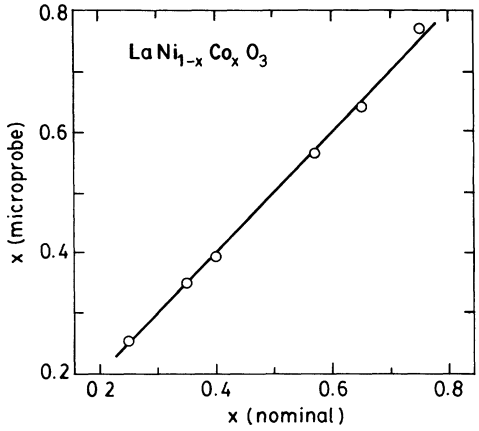

FIG. 2. Estimates of Co concentration, for various nominal values of x, using electron microphobe analysis (in the text, x always refers to the nominal value). These values were obtained by comparing the electron microprobe spectrum for a particular x, with those of $LaNiO_3$ and $LaCoO_3$.

ing $n_c \approx 0.6 \times 10^{22}/\text{cm}^3$. There are certain details about the *M-I* transition which may be specific to this system. These details can be found elsewhere.[10–12]

The crystal structure of $LaNiO_3$, is shown in Fig. 1. The relevant lattice parameters[11] are given in Table II. For all x, the structure remains essentially the same. The structure is very nearly cubic, with a slight rhombohedral (trigonal) distortion, with the pseudocubic angle 90.7°. The primitive rhombohedral cell, shown by thick lines in Fig. 1, contains two formula units.

III. EXPERIMENT

The material was made by the decomposition of coprecipitated carbonates. The details can be found elsewhere.[11] The decomposition product was given sufficient oxygen treatment to ensure proper stoichiometry and was characterized by x-ray diffraction and iodometry. The pressed and heat-treated pellets had a packing fraction better than 90%. The theoretical density, calculated using lattice parameters is ≈ 7 g/cm^3. The x-ray characterization ensured that the materials are of single phase and of the proper crystal structure. Iodometry fixed the oxygen stoichiometry to within 0.05 of 3. The pressed and sintered pellets were tested for composition by electron microprobe analysis. A comparison of the nominal composition and that obtained from the microphobe analysis is shown in Fig. 2. The estimated uncertainty in the Co (or Ni composition is $\sim 1-2\%$. From scanning-electron-microscope studies of the microstructure, typical grain sizes were found to be $\sim 1-2$ μm and the chemical composition was found to be homogeneous on this scale. The absolute resistivities were measured by the Van der Pauw method.[14] For low-temperature measurement, the sample was mounted on the cold finger of the cryostat using Apiezon N grease. The resistance was measured by a computer-automated low-frequency (20 Hz) ac method. The measurement currents used were in the range 1 μA to 1 mA, depending on the resistance and the temperature. The current was varied to check for any self-heating at lower temperatures. The precision in resistance measured is in the range 0.01–0.05 %. The absolute value of the resistivity is accurate to within 20%. Two commercially calibrated germanium resistance thermometers were used for temperature measurement below 40 K and a platinum thermometer for temperatures above 40 K. The temperature determination had a precision better than 0.1%. A combination of a pumped He cryostat, a ^{3}He cryostat and dilution refrigerator were used for scanning the complete temperature range.

TABLE II. Lattice parameters of $LaNiO_3$ and $LaCoO_3$. See Fig. 1.

Material	Symmetry	Pseudocubic lattice constants Edge (Å)	Angle
$LaNiO_3$	Rhombohedral	3.838	90°41′
$LaCoO_3$	Rhombohedral	3.826	90°40′

IV. RESULTS

The $\sigma(T)$ data for all the samples are shown in Fig. 3. The data clearly show the gradual yet distinct development of the insulating behavior as x is increased, starting from the metallic side at $x=0$. The change in sign of $d\sigma/dT$ at room temperature occurs at $x \approx 0.4$. However, for samples with $x < 0.4$, although $d\sigma/dT < 0$ at higher temperatures, there is a conductivity maximum occurring at $T < 100$ K and $d\sigma/dT > 0$ at lower temperatures. Even the pure metallic sample $LaNiO_3$, which at room temperature has a temperature coefficient of resistance

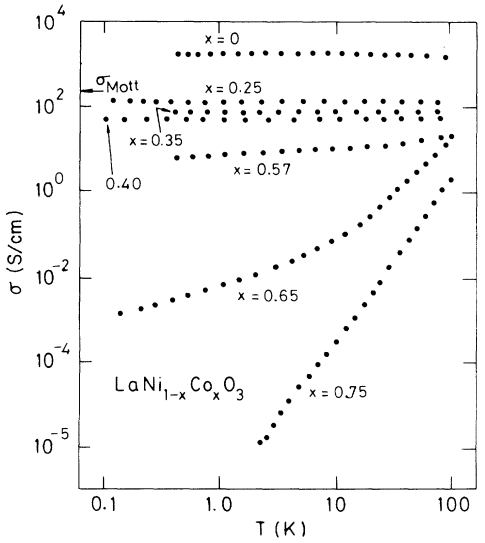

FIG. 3. $\sigma(T)$ for various x, as a function of temperature. The Mott minimum metallic conductivity σ_{Mott} is also shown in the figure.

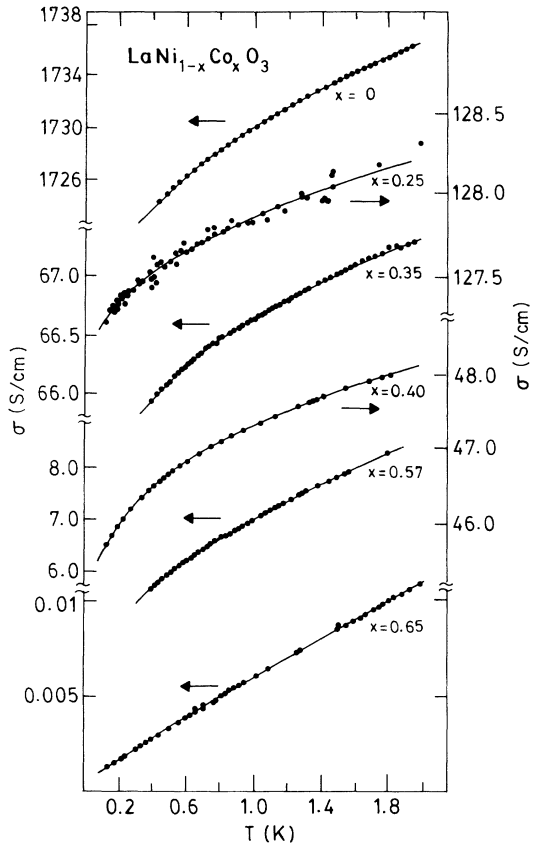

FIG. 4. Low-temperature conductivity ($T<2$ K) for various x. The lines show the power-law fit [Eq. (1)]. The absolute relative error for all the fits is less than 0.1%.

(TCR) $[(1/\rho)(d\rho/dT)]$ comparable to that of copper, shows a broad conductivity maximum at $T\approx 10$ K and below this temperature $d\sigma/dT>0$. (In Fig. 4 we have shown the low-temperature conductivity of the samples studied.) The fact that a particular sample can have a positive $d\sigma/dT$ at lower temperatures and a negative $d\sigma/dT$ at room temperature, even if the sample is distinctly metallic, points to the ambiguity of determination of metallicity from the sign of $d\sigma/dT$. Our analysis of $\sigma(T)$ (presented later on) for $T<2$ K has allowed us to estimate $\sigma(T=0)$ and from this we find that the critical composition $x_c\approx 0.65$ corresponding to $\sigma(T=0)=0$. It has recently been pointed out[15] that a better check of metallic or insulating behavior can be made through the evaluation of the derivative $d(\ln\sigma)/d(\ln T)$. If σ goes to a finite nonzero value as $T\rightarrow 0$ (i.e., if the system is metallic), $d(\ln\sigma)/d(\ln T)\rightarrow 0$ as $T\rightarrow 0$. On the other hand, if σ follows an exponential relation (for instance, due to variable-range hopping), $d(\ln\sigma)/d(\ln T)$ diverges as $T\rightarrow 0$. It is not necessarily true, however, that $d(\ln\sigma)/d(\ln T)$ should always diverge on the insulating side. For example, for cascade processes[16] on the insulating side it has been predicted that $\sigma(T)\propto T^s$ with $s\gg 1$. In this case, $d(\ln\sigma)/d(\ln T)\rightarrow$const$(s)$ for $T\rightarrow 0$. In Fig. 5 we have plotted $d(\ln\sigma)/d(\ln T)$ for a few samples close to the M-I transition on both the insulating side and the metallic side. For samples with $x\leq 0.57$, $d(\ln\sigma)/d(\ln T)$ goes to zero as T goes to zero, showing $\sigma(T=0)\neq 0$ for these samples. For the sample with $x=0.65$, $d(\ln\sigma)/d(\ln T)$ at the lowest temperatures tends to zero. But it should be pointed out that $d(\ln\sigma)/d(\ln T)$ is almost constant for $T<1$ K. This is a problem one faces with samples very close to the M-I transition; that it is difficult to distinguish a metal from an insulator. For the sample with $x=0.75$, which is an insulator, $d(\ln\sigma)/d(\ln T)$ diverges at lower temperatures. Figure 5 shows that the temperature dependence of $\sigma(T)$ below 10 K can be qualitatively different from the dependence above 10 K. It also shows that the limiting activation energy for an insulator of this type cannot be estimated from measurements done above 10 K. The $\sigma(T)$ for the

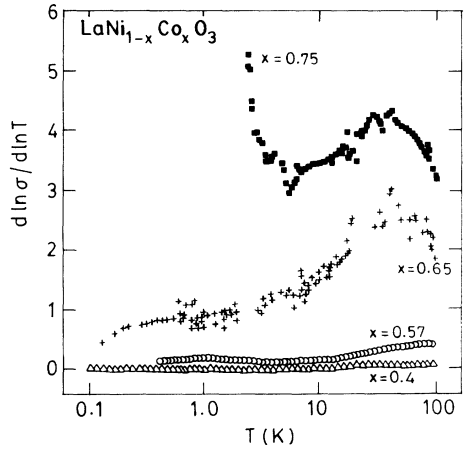

FIG. 5. $d(\ln\sigma)/d(\ln T)$ for samples on both sides of the M-I transition. For the clearly metallic samples ($x=0.4$ and 0.57), $d(\ln\sigma)/d(\ln T)\rightarrow 0$ as $T\rightarrow 0$, while for the insulating sample ($x=0.75$) it blows up at low temperatures.

sample with $x=0.75$ between 4 and 20 K seems to follow a power-law behavior with $s\approx 3.5$. But if we confine our attention to $T<4$ K, the best fit is obtained with the relation, $\sigma(T)\propto e^{-E_g/2k_BT}$, with $E_g=11.8$ K. The $x=0.65$ sample shows a behavior similar to that of the insulating sample above 10 K [for instance, the hump in $d(\ln\sigma)/d(\ln T)$ at $T\sim 30$ K]. But for $T<10$ K it shows a behavior which is qualitatively different. For all the samples σ_{RT} lies in the range 10^1-10^3 S/cm, although the σ of even the metallic samples, at low temperatures ($T\approx 0.4$ K), spans nearly six orders of magnitude. The Mott minimum metallic conductivity (σ_{Mott}) for this system is $\approx 2\times 10^2$ S/cm. Thus, for all the samples we have $\sigma_{RT}\sim\sigma_{Mott}$, implying $k_Fl\sim 1$ (l is the electron mean free path; σ_{Mott} defines the limit of Boltzmann transport). Since $\sigma<\sigma_{Mott}$ at lower temperatures for all the samples with $x\geq 0.25$, we have to conclude that most of the temperature dependence of σ in these materials for $T<100$ K comes from quantum corrections, be it localization or interaction effects.

The $\sigma(T)$ data ($T<2$ K) for the metallic samples ($x\leq 0.65$) were fitted to the relation

$$\sigma(T)=\sigma(0)+\delta\sigma(T)=\sigma(0)+\alpha T^m , \quad (1)$$

where $\sigma(0)$ is the extrapolated zero-temperature conductivity and $\delta\sigma(T)$ is the temperature-dependent part. The power-law fits for all the metallic samples are shown in Fig. 4. The fits are generally excellent with maximum deviation $\sim 0.05\%$ which is about the same order as the experimental uncertainty in the data. The fit parameters are given in Table III. In Fig. 6 we have plotted $\sigma(0)$ and the exponent m as a function of the composition x. On the metallic side and away from the transition ($x\leq 0.4$), m gradually decreases from 0.42 for $x=0$ to $m=0.31$ for $x=0.4$. As one approaches the transition, signaled by the rapid fall of $\sigma(0)$, m rises rapidly and at $x=x_c\approx 0.65$, $m\approx 1$.

The sample with $x=0.65$ sits very close to the *M-I* transition and for $T<2K$, $\sigma(T)$ is almost proportional to T. The $\sigma(0)$ for this sample ($\sim 3\times 10^{-4}$ S/cm) is orders of magnitude smaller than the $\sigma(0)$ of other samples. The material has a very low, but nonzero, $\sigma(0)$ and $d(\ln\sigma)/d(\ln T)\to 0$ as $T\to 0$ (see Fig. 5), indicating that it may be metallic.

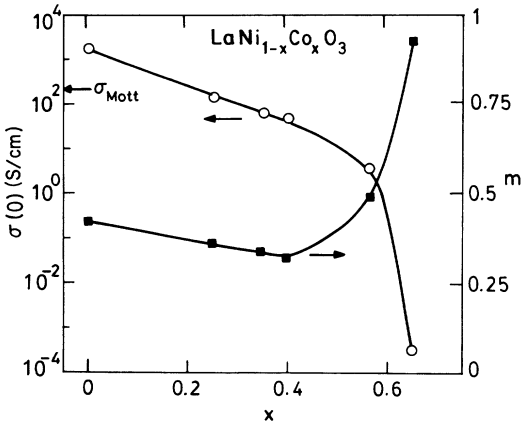

FIG. 6. The extrapolated conductivity $\sigma(0)$ obtained from fits to Eq. (1) (Fig. 4) as a function of Co concentration x, for the samples on the noninsulating side. σ_{Mott} is also indicated in the figure. Also shown is the power-law exponent m which becomes ≈ 1 at the transition ($x\approx 0.65$).

TABLE III. Fit parameters for the conductivity data (below 2 K) to Eq. (1) for the samples on the metallic side ($x\lesssim x_c=0.65$).

x	$\sigma(0)$ (S/cm)	α (S cm^{-1}K^{-m})	m
0.00	1710	19.7	0.43
0.25	127	1.00	0.36
0.35	64.1	2.58	0.34
0.40	43.8	3.48	0.31
0.57	3.51	3.52	0.53
0.65	3.12×10^{-4}	55.4×10^{-4}	0.93

V. DISCUSSION

We first try to explore the applicability of the theories of disordered electronic systems[5,17] to these materials in Secs. V A–V G. Following this, some other important issues are also discussed.

A. The temperature dependence of $\sigma(T)$ at low temperatures

We saw that at low temperatures, for $x\leq 0.57$, the power-law behavior of $\sigma(T)$ [Eq. (1)] is sublinear, and m, the power-law exponent, lies in the range 0.3–0.5. Such an exponent ($m\approx 0.5$) is expected to arise from electron-electron interactions.[5,17] In many materials,[18] m has been found to be 0.5, including the most studied Si:P (where the α can be positive or negative, depending on the electron concentration[19]). It has also been observed that for some materials $m<0.5$ and often $m\approx 0.3$.[6,8,20,21] If we are very close to the *M-I* transition an exponent $m\approx\frac{1}{3}$ can be expected.[8,17,20,22] However, the composition range where we find $m<0.5$ is away from the transition and one must look for a different explanation for this behavior. In what follows we show that a power-law behavior with $m<0.5$, for samples that are well within the metallic side ($x\leq 0.4$), can be accounted for, if we treat the interaction effects completely. To be specific, we take into account the Cooper-channel contribution[17] to the correction to conductivity in addition to the usual diffusion-channel contribution. The presence of the Cooper-channel contribution in conductivity has not been seen before, although it was predicted earlier.[17] We find such a contribution in our system. The quantum correction to σ due to interaction effects ($\delta\sigma_I$) contains two contributions:

$$\delta\sigma_I=\delta\sigma_D+\delta\sigma_C . \quad (2a)$$

The first term, $\delta\sigma_D$, is due to the diffusion channel (also called particle-hole channel), where one considers the effect of interaction of two particles with nearly equal

momenta, and the other term, $\delta\sigma_C$, is from the Cooper channel (also called particle-particle channel), which contains the effect of interaction of two particles with a small total momentum. The diffusion-channel contribution is given as[17]

$$\delta\sigma_D = 0.915\frac{e^2}{2\pi^2\hbar}\left(\tfrac{2}{3}-\tfrac{3}{4}\tilde{F}_\sigma\right)\left[\frac{k_BT}{\hbar D}\right]^{1/2}, \tag{2b}$$

where $\tilde{F}_\sigma$ is an effective interaction constant ($\tilde{F}_\sigma > 0$, typically $\tilde{F}_\sigma \sim 1$) and D is the diffusion coefficient. The Cooper-channel contribution is

$$\delta\sigma_C = -0.915\frac{e^2}{2\pi^2\hbar}\frac{1}{\ln(T_C/T)}\left[\frac{k_BT}{\hbar D}\right]^{1/2}. \tag{2c}$$

Here T_C is a parameter which depends on the dimensionless electron-phonon coupling constant λ, which measures the strength of the phonon-mediated electron-electron interaction.[17] For normal metals λ is positive, indicating an effective electron-electron repulsion. In this case $T_C \sim T_F e^{1/\lambda}$. In the weak-coupling limit, i.e., $\lambda \ll 1, T_C \gg T_F \gg T$. As a result, it can be seen from Eqs. (2) that the Cooper-channel contribution $\delta\sigma_C$ can be much smaller than the diffusion-channel contribution $\delta\sigma_D$. If $\delta\sigma_D$ is the dominant contribution to $\sigma(T)$, it gives rise to a $T^{1/2}$ dependence (i.e., $m=\frac{1}{2}$) for the conductivity at the low-temperature limit. However, it may happen that T_C is not too large, because of either a small T_F or strong electron-phonon coupling ($\lambda \sim 1$) resulting in $\delta\sigma_C$ becoming comparable to $\delta\sigma_D$ in magnitude. If $\delta\sigma_D > 0$ (i.e., $\tilde{F}_\sigma < \frac{8}{9}$) and $|\delta\sigma_D| > |\delta\sigma_C|$ ($\delta\sigma_C$ is always negative for a normal metal), the total interaction correction $\delta\sigma_I$ is positive. In such a case, the conductivity $\delta\sigma(T)$ can be easily mistaken to follow a power-law behavior [Eq. (1)] with $m < 0.5$ and $\alpha > 0$ at low-enough temperatures. This is because of the negative contribution from $\delta\sigma_C$ which, incidentally, does not follow a power law [Eq. (2c)]. We stress again that $m = 0.5$ only when $\delta\sigma_C$ is negligible. We show below that in oxides, both $\delta\sigma_C$ and $\delta\sigma_D$ are needed to account for the interaction corrections. For a normal disordered metal, if the low-temperature conductivity is found to follow a power-law behavior [Eq. (1)] with exponent (m) less than 0.5 (with $\alpha > 0$), the Cooper-channel contribution should be considered seriously, along with the diffusion-channel contribution.

The interaction effects which give a sublinear temperature dependence to σ dominate at lower temperatures, particularly below 1 K. We show below that the $\sigma(T)$ for $T < 10$ K, for samples that are deep in metallic side ($x \leq 0.4$), can be accounted for, to a high degree of accuracy, as arising from the interaction corrections $\delta\sigma_I$ [Eqs. (2)], and the weak-localization correction $\delta\sigma_{WL}$. The weak-localization correction depends on the phase-coherence length L_φ as follows:[17,23,24]

$$\delta_{WL} = \frac{e^2}{2\pi^2\hbar}\frac{1}{L_\varphi}. \tag{3}$$

The phase-coherence length L_φ is the distance an electron diffuses in the phase-relaxation time τ_φ so that $L_\varphi = (D\tau_\varphi)^{1/2}$. In three dimensions τ_φ is nearly the same as the inelastic lifetime[17] τ_{in} and thus it is expected that $\tau_\varphi^{-1} \propto T^p$ with $1 < p < 4$. But this is not correct if a temperature-independent scattering mechanism (see note below) is present. In this case we may write τ_φ^{-1} as a sum of terms arising from various scattering mechanisms as follows:[22]

$$\tau_\varphi^{-1} = \tau_{e-e}^{-1} + \tau_{e-ph}^{-1} + \tau_s^{-1} \tag{4}$$

where e-e stands for electron-electron scattering. e-ph represents electron-phonon scattering, and s denotes a temperature-independent scattering. For electron-electron scattering,[17,25,26] $\tau_{e\text{-}e}^{-1} \propto T^p$, where $p \approx 1.5$–2. For electron-phonon scattering,[24] $\tau_{e\text{-ph}}^{-1} \propto T^p$ where $p \approx 2$–4. In the absence of τ_s^{-1} term, $\tau_{e\text{-}e}^{-1}$ and $\tau_{e\text{-ph}}^{-1}$ can give rise to a t_φ^{-1}, which may resemble T^p with $1.5 < p < 4$, depending on the temperature and the relative strengths of the two terms. However, in the presence of temperature-independent scattering, the situation changes. [Note: The need for a temperature-independent scattering term (τ_s^{-1}) has also been found in metallic glasses.[27,28] Spin-flip scattering can be suggested as a mechanism responsible for the temperature-independent τ_s^{-1} term. However, we cannot say definitely if this spin-flip scattering is arising from local moments formed at Ni^{3+} sites or Co^{3+} sites. But identifying the finite τ_s^{-1} with spin-flip scattering has its problems, because weak-localization theory is applicable only when the scattering associated with spin flip is less than that due to inelastic scattering. Another mechanism that has been suggested for a temperature-independent dephasing term is the zero-point motion of the ions, from which the electrons scatter elastically.[27,28]]

Since τ_s^{-1} is a constant, τ_φ^{-1} can be written as

$$\tau_\varphi^{-1} = \tau_s^{-1}(1 + \tau_s A T^p), \tag{5}$$

where A is a constant determining the temperature-dependent inelastic scattering rate. Equation (5) implies that the phase-coherence length L_φ saturates at low temperatures. This can show up as a saturation of magnetoconductance at low temperatures.[17,29] Also, the low-temperature conductivity will have a constant term added to it corresponding to the limiting phase-coherence length [see Eq. (3)].

We have done magnetoconductance studies on our system in a field up to 7 T and down to 1.5 K. The analysis of magnetoconductance is involved and is discussed in a separate publication.[30] Here we use the relevant information that we need for this work. We found that (i) the magnetoconductance is positive and can be explained mainly as arising from the destruction of weak localization by the magnetic field, at least for samples well within the metallic region ($x \leq 0.4$), (ii) the magnetoconductance shows no temperature dependence below 4 K (i.e., saturation), and (iii) there is no evidence of a low-field negative magnetoconductance (i.e., spin-orbit scattering can be ruled out). If we interpret the low-temperature saturation of magnetoconductance as arising from the saturation of the temperature dependence of τ_φ^{-1} caused by the

TABLE IV. The limiting phase-coherence lengths (as $T \rightarrow 0$) as determined from magnetoconductance measurements.

x	Limiting phase-coherence length $\sqrt{D\tau_s}$ (Å)
0.25	163
0.40	142

temperature-independent τ_s^{-1} term, we can estimate the limiting phase-coherence length. $(D\tau_s)^{1/2}$ in terms of which the $\delta\sigma_{WL}$ can be written as [see Eq. (5)]

$$\delta\sigma_{WL}=\frac{e^2}{2\pi^2\hbar}\frac{1}{(D\tau_s)^{1/2}}(1+\tau_s AT^p)^{1/2} . \quad (6)$$

The $(D\tau_s)^{1/2}$ values obtained from the magnetoconductance data[30] are given in Table IV.

The complete expression for conductivity can now be written as

$$\sigma(T)=\sigma_0+\delta\sigma_I(T)+\delta\sigma_{WL}(T) , \quad (7)$$

with $\delta\sigma_I(T)$ and $\delta\sigma_{WL}(T)$ given by Eqs. (2) and (6), respectively.

The data for $T<10$ K, for samples well inside the metallic region ($x \leq 0.4$), were fitted to Eq. (7). A sample is well inside the metallic regime when $\delta\sigma(T) \ll \sigma_0$. We used the criterion $[\sigma(10\text{ K})-\sigma(0.4\text{ K})]/\sigma(0.4\text{ K})<0.1$, i.e., the quantum correction is $\sim 10\%$ of $\sigma(T)$. For $T<1$ K, the dominant temperature-dependent contribution to the correction to conductivity comes from $\delta\sigma_I(T)$ (see the parenthetical remarks at the end of the paragraph). We first fitted the data below 1 K to Eq. (2) using a nonlinear least-squares-fit program, to get rough estimates of D, $\sigma(0)$, $\tilde{F}_\sigma$, and T_C. These were then used as starting values for the full fit to the complete data below 10 K. In this fit we allowed full freedom to all six parameters, the additional parameters being A and p. One typical fit is shown in Fig. 7 and the fit parameters are presented in Table V. The inset to Fig. 7 shows the different contributions. If the fit is done without the τ_s^{-1} term in the weak-localization contribution, p turns out to be between two and three, while the interaction correction remains essentially unaffected; but the χ^2 is 30–80 % higher. As already noted, the evidence for the τ_s^{-1} term comes from the magnetoconductance data.[30] We point out that the analysis of $\sigma(T)$ data without the magnetoconductance data can lead to erroneous conclusions about the weak-localization correction. In the presence of strong $\delta\sigma_I$, it is difficult to find $\delta\sigma_{WL}$ unambiguously unless some prior information about L_φ (or τ_φ) that determines $\delta\sigma_{WL}$ are known. [However, if one takes the data below 2 K, it is possible to fix $\delta\sigma_I$ to a good extent if one ignores $\delta\sigma_{WL}$. (In fact, this is the way we got good starting values for the parameters for the full nonlinear fit.) This is possible in two cases: (i) $\delta\sigma_I \gg \delta\sigma_{WL}$ and (ii) $\delta\sigma_{WL}$ is constant.]

As the M-I transition is approached and the corrections become of the same order as or larger than σ, we see deviations from the above trend. For the sample with

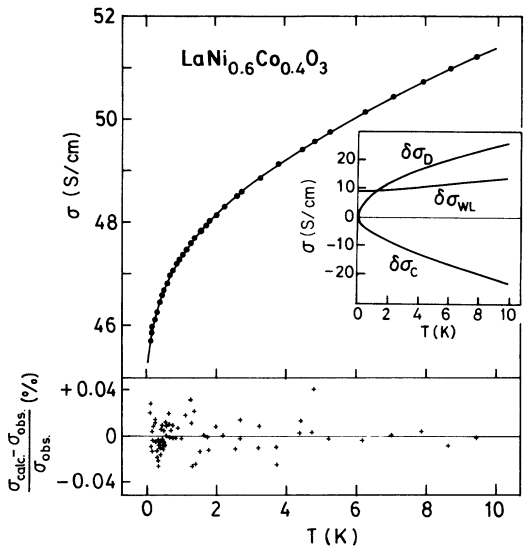

FIG. 7. $\sigma(T)$ for the $x=0.4$ sample. The curve passing through the data points shows the fit to Eq. (7). For clarity, not all the data points are shown. The percentage error of the fit is shown at the bottom of the graph (here all points are shown). The average percentage error of the fit is 0.02%. The various contributions to the fit (see text) are indicated in the inset.

TABLE V. Fit parameters for the conductivity data (below 10 K) to Eq. (7). For the sample with $x=0.35$, $\sqrt{D\tau_s}$ is also a fit parameter since the magnetoconductance was not measured on this sample. The temperatures and conductivities of the data set lie in the ranges (T_{min}, T_{max}) and $(\sigma_{min}, \sigma_{max})$, respectively. N is the total number of data points for each sample. χ^2 is defined as $\chi^2=(1/N)\sum(\sigma_{measured}-\sigma_{fit})^2$.

Parameter	Composition $x=0.25$	$x=0.35$	$x=0.40$
Characteristics of the data set			
T_{min} (K)	0.12	0.4	0.13
T_{max} (K)	9.4	9.2	9.43
σ_{min} (S/cm)	127.2	65.9	45.7
σ_{max} (S/cm)	130.8	70.2	51.2
N	98	197	80
Characteristics of the fit			
χ^2	1.7×10^{-3}	1.1×10^{-4}	4.1×10^{-5}
Avg. error	0.04%	0.02%	0.02%
Fit parameters			
σ_o (S/cm)	119.1	56.0	35.7
D (cm^2/s)	1.31×10^{-2}	1.23×10^{-2}	0.857×10^{-2}
$\tilde{F}_\sigma$	0.73	0.66	0.64
T_C (K)	34275	6047	4130
τ_s (s)	2.02×10^{-10}	1.65×10^{-10}	2.36×10^{-10}
A	3.11×10^{8}	3.17×10^{8}	1.85×10^{8}
p	1.40	1.38	1.48
Derived parameters			
m_r	25	27	39
ξ (Å)	20	43	68
λ	0.35	0.90	1.38

$x=0.57$, we find that the exponent m is on the verge of a rapid rise, signaling a change of behavior. For this sample, the correction $\delta\sigma(T)$ is of the order of $\sigma(T)$ for $T\sim 10$ K. To be specific $[\sigma(10\text{ K})-\sigma(0.4\text{ K})]/\sigma(0.4\text{ K})=0.8$). As a result, the quantum correction theories, which were developed for small corrections, are not expected to be valid here. This sample is not in the weak-localization regime. But $\sigma(T)$ still follows a power law (for $T<2$ K) with $m\approx 0.5$. (On a naive application of the interaction theory, one would conclude that for this sample the diffusion channel is dominating the conductivity.) What is more intriguing, the power-law behavior is seen in samples even nearer to the transition ($x=0.65\approx x_c$) with $m\approx 1$, and on the insulating side with $m>1$.

As one approaches the strong-localization regime, the correlation length (ξ) begins to diverge.[5] Generally, in this limit, one expects that the relevant time scale is the thermal smearing time τ_{th} ($\sim\hbar/k_BT$) and this leads to a $\sigma\propto T^{1/3}$ behavior.[17] This has been observed in a few cases.[6,8] However, in our case the exponent $\rightarrow 1$ as the *M-I* transition is approached. At present, we have no explanation for this behavior.

The important conclusions we draw from the above analysis are as follows.

(i) Away from the *M-I* transition the theories of disordered electronic systems can describe the low-temperature conduction provided proper attention is paid to all the correction terms and the various dephasing mechanisms. In particular, the unambiguous observation of the Cooper-channel contribution is an important point.

(ii) Nearer the transition the theories do not seem to work.

B. The physical justification of parameters

The various parameters obtained from the conductivity data (given in Table V) represent physical quantities whose magnitudes can be estimated or can be used to estimate other quantities of physical significance. We now take a look at the parameters in the order of their appearance in Eq. (7). In particular, we would like to see if the parameters obtained fall within physically justifiable limits.

(i) σ_o. This quantity is related to the $\sigma(0)$ of Eq. (1) as follows:

$$\sigma_o=\sigma(0)-\frac{e^2}{2\pi^2\hbar}\frac{1}{(D\tau_s)^{1/2}}\ . \tag{8}$$

In Fig. 6 we have plotted $\sigma(0)$ as a function of composition x. σ_o is related to the correlation length (ξ), $\sigma_o\sim 0.1e^2/\hbar\xi$. We find $\xi\approx 1.4$ Å for $LaNiO_3$ (assuming no spin-flip scattering) and $\xi\approx 69$ Å for the $x=0.4$ sample. If, for the $x=0.57$ and $x=0.65$ samples, we take $\sigma(0)$ as the upper limit for σ_o, we find $\xi\sim 700$ Å for $x=0.57$ and $\xi\sim 0.8$ mm for $x=0.65$. A $\xi\sim 0.8$ mm for a sample of grain size ~ 1–2 μm is definitely unphysical and we thus doubt that the $\sigma(0)$ observed for this sample ($x=0.65$) has any meaning. When ξ becomes larger than a few micrometers [i.e., for $\sigma(0)\sim\sigma_o<1$ S/cm], crystal grain effects, sample inhomogeneities, and other such extraneous factors may influence the results. For samples so close to the critical region, we think, special attention must be given to all these factors. (An example of the effect of small compositional inhomogeneities near the *M-I* transition is given in Ref. 8.) Our current sample preparation and characterization techniques are definitely unsuitable for studying samples so close to the transition region. We therefore cannot ascribe any physical meaning to the $\sigma(0)$ of the sample with $x=0.65$. For other samples, with $x\leq 0.57$ we feel that the σ_o represents the conductivity prescribed by the correlation length ξ, the estimates of which seem reasonable.

(ii) D. The values of D obtained from the fit for the three samples with $x=0.25$, 0.35, and 0.40 are 0.013, 0.012, and 0.009 cm^2/s, respectively. We now show that these numbers are indicators of an enhanced effective mass for the electrons in the system. The diffusion coefficient D is related to the disorder parameter k_Fl in the following way:

$$D=\frac{\hbar}{3m_{\text{eff}}}k_Fl\ . \tag{9}$$

If one expresses D in cm^2/s, Eq. (9) can be conveniently written as

$$D\approx k_Fl/(3m_r)\ , \tag{10}$$

where m_r is the ratio of effective mass to the bare-electron mass. k_Fl for $LaNiO_3$ is ~ 2.5, and for the other samples, with $x\leq 0.4$, we believe that $k_Fl\sim 1$. m_r for $LaNiO_3$ is ≈ 11 (see Table I) and, with the addition of Co into the system, it is very likely that the conduction band becomes narrower and m_r increases. If we estimate m_r from Eq. (10) (assuming $k_Fl\sim 1$), we find that the effective mass m_r for the $x=0.25$ sample is ~ 25 and that for the $x=0.4$ sample is ≈ 39 (see Table V). These estimates show that as the *M-I* transition is approached ($k_Fl\sim 1$), the fall in D can come from a rising effective mass of the electron. The heavy effective mass could, presumably, be attributed to an enhanced electron-phonon interaction or to the band becoming narrow due to a reduced overlap of neighboring orbitals.

(iii) $\tilde{F}_\sigma$. The effective interaction constant is more or less constant around 0.7. $\tilde{F}_\sigma$ depends on the interaction constant F, which, in turn, depends on the screening length and other details of the static screened Coulomb potential between electrons.[5,17] Within the Thomas-Fermi approximation[31] one has

$$F=(1/y)\ln(1+y)\ , \tag{11}$$

where $y=(2k_F/\kappa)^2$, κ being the inverse screening length; $\kappa=[e^2g(E_F)/\epsilon_0]^{1/2}$, where $g(E_F)$ is the density of states at the Fermi level and ϵ_0 is the permittivity of free space. $\tilde{F}_\sigma$ and F are related by the following relation:

$$\tilde{F}_\sigma=-\frac{32}{3F}[1+3F/4-(1+F/2)^{3/2}]\ . \tag{12}$$

For $LaNiO_3$, the density of states at the Fermi level,[3]

$g(E_F)\approx 1.1\times 10^{23}$ eV^{-1} cm^{-3} (Table I) and we find $\kappa=4.5\times 10^{8}$ cm^{-1}. k_F for $LaNiO_3$ is 0.8×10^{8} cm^{-1}. From Eqs. (12) and (11) we obtain $\tilde{F}_\sigma=0.88$, which is reasonably close to the fit parameter obtained for the metallic samples. However, a word of caution is called for. It must be mentioned that a good estimate does not necessarily mean that these numbers are physically meaningful as these are estimates based on the simple Thomas-Fermi approximation which, itself, can be doubted in these materials with d-electron conduction.

(iv) T_C. The T_C that determines the Cooper-channel contribution arises from phonon-mediated electron-electron interaction.[17] In our case we used it as a fit parameter. For cases where the interaction is attractive (i.e., the dimensionless electron-phonon coupling constant $\lambda<0$), leading to a superconducting state, T_C is identified with the superconducting transition temperature and is given by $T_C\sim\Theta_D e^{1/\lambda}$, where Θ_D is the Debye temperature. [We have seen that in a disordered-oxide superconductor of low T_C (~ 2 K) the shape of the conductivity curve near T_C can be described very well by a Cooper-channel contribution[32] using the observed T_C.] For cases where the interaction is repulsive ($\lambda>0$, the system does not go superconducting and T_C is just a formal parameter given by $T_C\sim T_F e^{1/\lambda}$, where T_F is the Fermi temperature. As λ increases, T_C decreases. Typically for metals, $\lambda\sim 0.1$. We find, from the T_C (see Table V) obtained from the fit to the experimental data (assuming an average $T_F=2000$ K), that λ increases from 0.3 to 1.4 as x is increased. The rapid drop in T_C on doping thus comes mainly from an increase in λ, with some help from a decreasing T_F. The increase in λ points to the strengthening of the electron-phonon interaction in these materials. This may lead to an enhanced electron effective mass, as has been seen before. (We feel that the electron-phonon interaction may not be the only cause of a strong Cooper-channel contribution. We are of the opinion that the Cooper-channel contribution in oxides—including the high-T_C oxides—are strong, in general.)

(v) A and p. The temperature-dependent part of the phase-relaxation rate for our system ($=AT^p$) can be estimated from the fit parameters. For the samples with x ranging between 0.25 and 0.4, the exponent p lies in the range of 1.4–1.5. This value of p suggests electron-electron scattering as the dominant scattering mechanism. The predicted exponent for this process lies between 1.5 and 2. The expression we use for estimating the scattering rate is[25]

$$\tau_{e\text{-}e}^{-1}=\frac{\pi}{8\hbar}\frac{(k_B T)^2}{E_F}+\frac{\sqrt{3}}{2\hbar}\frac{1}{(k_F l)^{3/2}}\frac{(k_B T)^{3/2}}{\sqrt{E_F}}\ . \qquad (13)$$

Evidently, for a small $k_F l$, the second term dominates at lower temperatures. The values for $\tau_{e\text{-}e}^{-1}$ [obtained from Eq. (13)] are compared to the temperature-dependent part of the phase-relaxation rate [see Eq. (5)] in Fig. 8. The agreement with the observed behavior is excellent if we take $k_F l=5$ in (13). Also shown in the figure, for comparison, is the electron-electron scattering rate for $k_F l=1$.

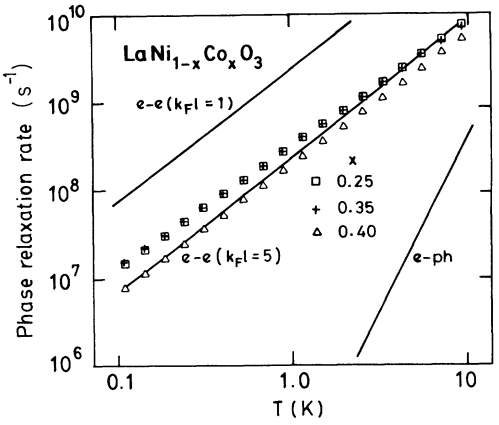

FIG. 8. The temperature-dependent part of the phase relaxation rate τ_φ^{-1} for the three samples that are well inside the metallic region. The solid lines are the calculated inelastic lifetimes for electron-electron scattering (e-e) and electron-phonon scattering (e-ph).

If electron-phonon scattering is the dominant inelastic process, it is expected that p lies between 2 and 4. We have also plotted in Fig. 8 the scattering rate calculated for this case using the expression[24]

$$\tau_{e\text{-ph}}^{-1}\approx \text{const}\times l(k_B T)^4/(\hbar^2 m_{\text{eff}} M c^5)\ , \qquad (14)$$

where M is the ion mass and c is the speed of sound; const≈ 4. This expression is valid in the low-temperature limit $k_B T\ll \hbar c/l$. We find that the estimated electron-phonon scattering rate is far too small. Only for $T\gg 20$ K does it become comparable to, or larger than, $\tau_{e\text{-}e}^{-1}$.

C. Length scales

From the weak-localization term $\delta\sigma_{\text{WL}}$, we find the phase-coherence length L_φ [Eqs. (3) and (6)]. In Fig. 9 we plot L_φ as a function of temperature for the doped metallic samples ($x\le 0.4$) and in the same graph we show the correlation length ξ. For all the samples at $T>10$ K, $L_\varphi\to\xi$, but at lower temperatures $L_\varphi>\xi$. This provides the justification for our use of the weak-localization theory which is applicable for the regime where $L_\varphi\gg\xi$ (i.e., far from the critical region). Please note also the saturation of L_φ at lower temperatures which leads to the saturation of magnetoconductance below 4 K.[30] Figure 9 shows that it is not justifiable to use concepts and theories contained in Eqs. (2) and (3) for analyzing data above ~ 10 K. Also, for the material with $x=0.57$, ξ (~ 700 Å) $>L_\varphi$, implying that we are in the critical regime where the weak-localization theories should break down. We can see that for $x\ge 0.57$, there is a marked change in the temperature dependence (Table III, Fig. 6) with a rapid increase of the power-law exponent, signaling the onset of a change of regime. As pointed out earlier, in the regime $\xi>L_\varphi$, one observes a conductivity which varies as $T^{1/3}$ at low temperatures in

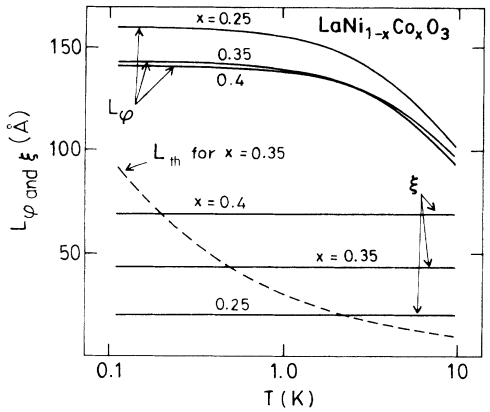

FIG. 9. The phase-coherence length L_φ as a function of temperature for the three samples well inside the metallic regime. Note the saturation at lower temperatures. The correlation length ξ is also shown. The thermal diffusion length $L_{\rm th}$ for the $x=0.35$ sample is indicated. $L_{\rm th}$ for the other two samples are nearly the same.

certain cases.[8,21,22] However, in our system we find a different behavior in the critical regime.

Another length scale of importance in a disordered metal is the thermal-diffusion length, $L_{\rm th}$. It is defined as $L_{\rm th}=\sqrt{\hbar D/k_B T}$. The theory of weak localization is strictly applicable only in the range, $L_{\rm th}\gtrsim\xi$.[17] As an example, in Fig. 9, we show the thermal-diffusion length for the sample with $x=0.35$. The other two samples also have almost the same $L_{\rm th}$. We see that our samples are really borderline cases as far as weak localization is concerned. The analysis presented above shows the extent to which the current theories of disordered electronic systems are applicable to (and can explain) the low-temperature conductivity of rather complex systems. (It also shows the caution we must exercise in applying these theories.)

D. The effect of polycrystallinity

At this point, it would be of interest to consider the effect of polycrystallinity on the data. Our samples are very nearly cubic and the packing fraction is better than 90%. Therefore, it is more probable that the measured conductivity will not be off by more than a factor of 2 from the true value. This becomes clear when one considers well-made samples of the high-T_C superconductors. Even in such highly anistropic systems, the observed σ in the well-made polycrystalline samples differs only by a factor of 2–3 from the in-plane conductivity.[33] Also, in our case, the relevant length scales, as we found earlier for the samples far away from the transition, are much less than the grain size (1–2 μm). For this reason, we believe, the temperature dependence of the conductivity will be the same as that of a single crystal, if one could be made; thus, most of our analysis and conclusions will remain unaffected. (Attempts to grow single crystals of $LaNiO_3$ by the flux method generally leads to La_2NiO_4.[34])

The uncertainty in the conductivity will affect the absolute values of $\sigma(0)$ and D. An underestimated conductivity leads to an overestimated diffusion coefficient. If the measured conductivity is less by a factor of 2, the diffusion coefficient (D) estimated from the data will be greater by a factor of 4 (this is because, in the expressions for the correction to conductivity, D enters as $1/\sqrt{D}$). This shows the extent of uncertainty one would expect from the use of polycrystalline samples. However, for samples near the critical region (very large ξ), we think, the grain size and other related effects will be important and investigations using polycrystalline samples will be of little quantitative (or even qualitative) significance.

E. The case of $LaNiO_3$

For $LaNiO_3$, the total change in conductivity[4] between 0.4 and 10 K is only 1.5%. But, since the conductivity itself is large ($\sigma_o=1710$ S/cm), the total change has a magnitude ≈ 25 S/cm, which is larger than those for the other samples. The best fit was obtained using the relation $\sigma(T)=\sigma_o+a\sqrt{T}-bT^p$; the last term ($bT^p$) could be considered as a correction due to normal scattering.[4] The fit parameters are $\sigma_o=1712$ S/cm, $a=18$, $b=0.27$, and $p=1.8$. The $\sqrt{T}$ term can be identified with $\delta\sigma_D$ [see Eq. (2b)]. In that case, using the fit value of a, we find, $D=0.0024$ cm^2/s (with $\tilde{F}_\sigma$ taken to be 0.6). This is much lower than the D (0.087 cm^2/s) estimated from the Einstein relation for conductivity $\sigma=e^2D\partial N/\partial\mu$ [here we take $\partial N/\partial\mu=g(E_F)$ because the conductivity corrections are small[17]]. This is a rather puzzling observation. We are not sure whether or not any other process is contributing to the conductivity of $LaNiO_3$ or if even in this case, due to interaction effects, it is wrong to use $\partial N/\partial\mu=g(E_F)$.

What could be responsible for the large disorder in $LaNiO_3$? In other words, what is the nature of this disorder. We suggest that oxygen deficiency is responsible for the disorder in $LaNiO_3$. As pointed out in the experimental section of the present paper, oxygen stoichiometry can be off by as much as 0.05 from 3, which is approximately 2%. We believe that this introduces sufficient disorder to give a large residual resistivity as well as a $T^{1/2}$ term in the low-temperature conductivity and a square-root dip in the tunneling conductance (Ref. 4). Anyway, our investigations warrant a detailed study of the exact nature of the disorder in this type of oxide metals.

F. The sample with $x=0.65$

This particular sample has a rather curious behavior. For 0.05 K $<T<$ 10 K, $\sigma(T)$ follows an almost linear relation. Also for this sample the zero-temperature conductivity σ_o is unusually low, giving unphysical values for the correlation length ξ. This sample lies at the critical region, and so ξ is expected to be large. The $d(\ln\sigma)/d(\ln T)$ (see Fig. 5) suggests metallicity for this sample, since it tends to decrease towards zero as $T\to 0$. It is certain that for this material the quantum correction

theories, as they stand now, will not be applicable. So far, we have not found a report of linear behavior at such low temperatures (there are reports of $\sigma \propto T$ at higher temperatures in some oxides, but our past investigation has shown that these samples show a different behavior at lower temperatures[7,8]). We cannot provide any explanation for this behavior. But we believe that in the critical region, sample inhomogeneity and other such effects have to be considered.

G. The high-temperature behavior

The resistivity of $LaNiO_3$ is found to be proportional to T, for $T > 100$ K, like many other good metals. Any sample with $x < 0.4$ has a positive TCR at room temperature; it also has a minimum in the resistivity, which shifts to higher temperature for increasing values of x. The higher-temperature positive TCR in these materials could be attributed to the usual scattering of electrons (which gives a positive TCR in good metals). For samples with $x \geq 0.4$, TCR at room temperature is negative ($d\sigma/dT > 0$). We could not find any simple relation to describe the high-temperature ($T > 20$ K) conductivity of these materials. The crossover from the high-temperature to low-temperature behavior for the metallic samples occurs at $T \sim 20$ K, where $\xi \sim L_\varphi$. It has been suggested[6,8] that since at higher temperatures $\xi > L_\varphi$, one would expect a situation similar to the critical region (where ξ diverges and becomes the largest length scale). In that case $\sigma \propto (\tau_\varphi^{-1})^{1/3}$, as has been pointed out before.[22] At high temperatures τ_φ^{-1} is dominated by electron-phonon scattering ($\tau_\varphi^{-1} \propto T^p$, $2 < p < 4$); as a result $\sigma \propto (\tau_\varphi^{-1})^{1/3} \propto T^n$ with $n \approx 0.67-1.34$. This has been observed in certain oxides.[6,8] We tried to explain the observed high-temperature behavior within the above framework, but were unable to do so. In fact, the temperature dependence of $\sigma(T)$ at higher temperatures remains an unsolved question.

The exact nature of the M-I transition in most of the oxides appears to be rather involved and unexplained. The interplay of interaction and localization effects is bound to make a disorder-driven transition quite complex. Other complications are a narrow band width, a large effective mass (because the band is formed from hybridized transition-metal orbitals), and a high electron density. Nevertheless, it is intriguing that away from the transition (in our case, samples with $x \leq 0.4$), the low-temperature behavior ($T < 10$ K) seems to be explicable, considering only the weak-localization and interaction effects arising from disorder, treating them as additive. By hindsight, this could probably be expected, because the interaction theory is applicable even when the disorder is large ($k_F l \leq 1$),[17] although weak-localization theory works well only for $k_F l \gg 1$. But in our case the interaction corrections have turned out to be dominant, thus justifying our analysis. Perhaps all these point towards the very general nature of the underlying Fermi-liquid theory.

With the approach of the transition (in our case, samples with $x \geq 0.57$) or at high temperatures where the corrections are not small, we do find that the theories are not applicable in the present form. Here, probably, the interaction and localization effects are not simply additive, and so are inseparable. We point out again that, even well within the metallic state (i.e., away from the transition), the high-temperature behavior cannot be explained. Perhaps a few more studies on such systems over a large temperature range will be required to see if any general trend emerges. However that may turn out, one point is fairly clear from the present study: at low temperatures the conductivity of these oxides will show considerable contributions coming from interaction effects. In our case the contribution is so great that even in pure $LaNiO_3$ one sees the interaction effects.

VI. CONCLUSION

We tried to analyze our data in some detail to obtain as much quantitative information as possible without introducing too many assumptions. Although the perovskite-structure oxide system we studied is supposed to be rather simple, it turned out to have its own complexity. Our present investigation clearly showed the following.

(i) In spite of the complexity of the system, in the regime of small corrections, the present theories of quantum corrections seem to explain the data, provided that proper attention is paid to the details.

(ii) We identified a Cooper-channel contribution in a nonsuperconducting metallic oxide. We have also pointed out the importance of this term in determining the power-law behavior of $\sigma(T)$ at lower temperatures.

(iii) We have also shown that, as we leave the regime of small corrections and the metal-insulator transition is approached, there is really no theory that can explain the data. This is also the case at higher temperatures. The results of our investigation of the low-temperature electrical conduction in the perovskite type of oxides on the metallic side of the M-I transition should be useful to further work on this subject.

ACKNOWLEDGMENTS

The authors thank T. V. Ramakrishnan and N. Kumar for many helpful discussions. The help of N. Y. Vasanthacharya in the initial stages of the work and of S. Banerjee in some of the low-temperature measurements are noted with thanks. One of us (K.P.R.) thanks CSIR for partial support. The work was supported by DST (Government of India).

[1] *Metallic and Non-metallic States of Matter,* edited by P. P. Edwards and C. N. R. Rao (Taylor and Francis, London, 1985).

[2] K. P. Rajeev, N. Y. Vasanthacharya, A. K. Raychaudhuri, P. Ganguly, and C. N. R. Rao, Physica C **153 - 155**, 1331 (1988).

[3] T. F. Rosenbaum and S. A. Carter, J. Solid State Chem. **88**, 94 (1990).

[4] K. P. Rajeev, G. V. Shivashankar, and A. K. Raychaudhuri, Solid State Commun. **79**, 591 (1991).

[5]P. A. Lee and T. V. Ramakrishnan, Rev. Mod. Phys. **57**, 287 (1985).
[6]Z. Ovadyahu, J. Phys. C: Solid State Phys. **19**, 5187 (1986).
[7]M. A. Dubson and D. Holcomb, Phys. Rev. B **32**, 1955 (1985).
[8]A. K. Raychaudhuri, Phys. Rev. B **44**, 8572 (1991).
[9]E. Abrahams, P. W. Anderson, D. C. Licciardello, and T. V. Ramakrishnan, Phys. Rev. Lett. **42**, 673 (1979).
[10]N. Y. Vasanthacharya, P. Ganguly, and C. N. R. Rao, J. Solid State Chem. **54**, 400 (1984).
[11]N. Y. Vasanthacharya, Ph.D thesis, Indian Institute of Science (1985).
[12]N. Y. Vasanthacharya, P. Ganguly, and J. B. Goodenough, J. Phys. C **17**, 2745 (1984).
[13]J. B. Goodenough, Prog. Solid State Chem. **5**, 145 (1972).
[14]L. J. Van der Pauw, Philips Res. Rep. **13**, 1 (1958).
[15]A. Möbius, Solid State Commun. **73**, 215 (1990).
[16]M. Pollak, in *Electron-Electron Interactions in Disordered Systems,* edited by A. L. Efros and M. Pollak (North-Holland, Amsterdam, 1985).
[17]B. L. Altshuler and A. G. Aronov, in *Electron-Electron Interactions in Disordered Systems* (Ref. 16).
[18]Uwe Thomanschefsky, Ph. D. thesis, Cornell University, 1990.
[19]R. F. Milligan, T. F. Rosenbaum, R. N. Bhatt, and G. A. Thomas, in *Electron-Electron Interactions in Disordered Systems* (Ref. 16).
[20]Y. Imry and Z. Ovadyahu, J. Phys. C **15**, L327 (1982).
[21]M. C. Maliepaard, M. Pepper, R. Newbury, and G. Hill, Phys. Rev. Lett. **61**, 369 (1988).
[22]Y. Imry, J. Appl. Phys. **52**, 1817 (1981).
[23]P. W. Anderson, E. Abrahams, and T. V. Ramakrishnan, Phys. Rev. Lett. **43**, 718 (1979).
[24]S. Chakravarty and A. Schmid, Phys. Rep. **140**, 193 (1986).
[25]A. Schmid, Z. Phys. **271**, 251 (1974).
[26]G. Bergmann, Z. Phys. B **48**, 5 (1982).
[27]R. Richter, Ph. D. thesis, McGill University, Canada, 1988.
[28]N. Kumar, D. V. Baxter, R. Richter, and J. O. Strom-Olsen, Phys. Rev. Lett. **59**, 1853 (1987).
[29]A. Kawabata, Solid State Commun. **34**, 431 (1980).
[30]K. P. Rajeev and A. K. Raychaudhuri (unpublished); K. P. Rajeev, Ph. D. thesis, Indian Institute of Science, 1991.
[31]H. Fukuyama in *Electron-Electron Interactions in Disordered Systems* (Ref. 16).
[32]S. Banerjee, K. P. Rajeev, and A. K. Raychaudhuri (unpublished).
[33]H. E. Fischer, S. K. Watson, and D. G. Cahill, Comments Condens. Matter Phys. **14**, 65 (1988).
[34]P. Ganguly (private communication).